A SANS Investigation of Reverse (Water-in-Oil) Micelles of Amphiphilic Block Copolymers

Birgitta Svensson* and Ulf Olsson

Physical Chemistry 1, Center for Chemistry and Chemical Engineering, Lund University, P.O.B. 124, SE-221 00 Lund, Sweden

Paschalis Alexandridis

Department of Chemical Engineering, State University of New York at Buffalo, Buffalo, New York 14260-4200

Kell Mortensen

Condensed Matter Physics and Chemistry Department, Risø National Laboratory, DK-4000 Roskilde, Denmark

Received January 20, 1999; Revised Manuscript Received July 8, 1999

ABSTRACT: Poly(ethylene oxide)−poly(propylene oxide)−poly(ethylene oxide) (PEO−PPO−PEO) block copolymers, commercially available as Poloxamers or Pluronics, are unique in forming ordered cubic phases consisting of reverse (water-in-oil) micelles. We set out to study the microstructure (form and dimension) as the reverse micelles order (from a micellar solution to a cubic lattice) with increasing block copolymer volume fraction and with increasing block copolymer molecular weight. The technique we used was small-angle neutron scattering (SANS) with solvent contrast variation. We selected four block copolymers with known phase behavior in water and *p*-xylene (Pluronics L44, L64, P84, and P104, all with the same PEO/PPO ratio and molecular formula $(EO)_x(PO)_y(EO)_x$, where $x = 10$, 13, 19, 27 and $y = 23$, 30, 43, 61, respectively) and worked in a dilution line with fixed water to copolymer content (1.2 mol of water per mol of EO). The temperature effect (22 and 45 °C) was also studied. The scattering behavior indicates that the micelles are approximately spherical but polydisperse. We used a two-sphere model where we assumed that all the PEO and the water are in the core of the micelle and that PPO forms a *p*-xylene-solvated shell. The micellar radius then depends on the molecular weight and the temperature and is approximately constant with concentration. The structure of the reverse micelles is also compared to that of normal (oil-in-water) micelles.

1. Introduction

The self-assembly of amphiphilic block copolymers in selective solvents has attracted increasing attention in recent years. (For recent reviews see for example refs 1 and 2 and references therein.) A commonly studied class of amphiphilic block copolymers are polyoxyalkylene copolymers of the type *block*-poly(ethylene oxide)-*block*-poly(propylene oxide)-*block*-poly(ethylene oxide), often denoted as $(EO)_x(PO)_y(EO)_x$, where x is the number of EO segments in the end block and y is the number of PO segments in the middle block. The PEO−PPO−PEO block copolymers are known under the generic name Poloxamers and the trade names Pluronic (BASF) or Synperonics (ICI). These block copolymers are available at different molecular weights and different relative block sizes. In aqueous solutions and at ambient temperatures, the PEO−PPO−PEO block copolymers can self-associate into micelles where the more hydrophobic PPO block forms a micellar core covered by a hydrated corona of the more hydrophilic PEO blocks.[3−7] At higher concentrations lyotropic liquid crystals are formed, and the binary phase diagrams with water are similar to those of short-chained nonionic surfactants.[8−10]

While the aqueous systems have been rather well studied, less is known about the self-association behavior in apolar solvents for these PEO−PPO−PEO block copolymers. They are generally soluble in aromatic solvents such as xylene but without forming aggregates. Block segregation is however dramatically increased by the addition of small amounts of water, leading to micelle formation.[11−13] This seems to illustrate the complex solubility behavior of PEO that can undertake both hydrophilic and hydrophobic conformations.[14] In the presence of a small amount of water, the PEO blocks become effectively more hydrophilic, and the block copolymers form reverse micelles. A similar behavior is also seen for nonionic surfactants of the ethylene oxide type.[15,16]

In our group we have recently investigated a number of ternary phase diagrams of PEO−PPO−PEO block copolymers in selective solvents such as water and *p*-xylene. In particular, we have studied a sequence of four PEO−PPO−PEO block copolymers with the same architecture and block composition (approximately 40 wt % PEO and 60 wt % PPO), but with different molecular weights.[17−19] The trade names and the molecular formulas are as follows: Pluronic L44, $(EO)_{10}(PO)_{23}(EO)_{10}$; Pluronic L64, $(EO)_{13}(PO)_{30}(EO)_{13}$; Pluronic P84, $(EO)_{19}(PO)_{43}(EO)_{19}$; Pluronic P104, $(EO)_{27}(PO)_{61}(EO)_{27}$, and their nominal molecular weights are 2200, 2900, 4200, and 5900, respectively. Our investigations have demonstrated the strong molecular weight dependence of the formation of lyotropic mesophases.[17−19] The lowest molecular weight (Pluronic L44) system exhibits a region of lamellar phase and a small region of reverse

* To whom correspondence should be addressed. e-mail Birgitta.Svensson@fkem1.lu.se.

10.1021/ma990079w CCC: $18.00
Published on Web 09/14/1999

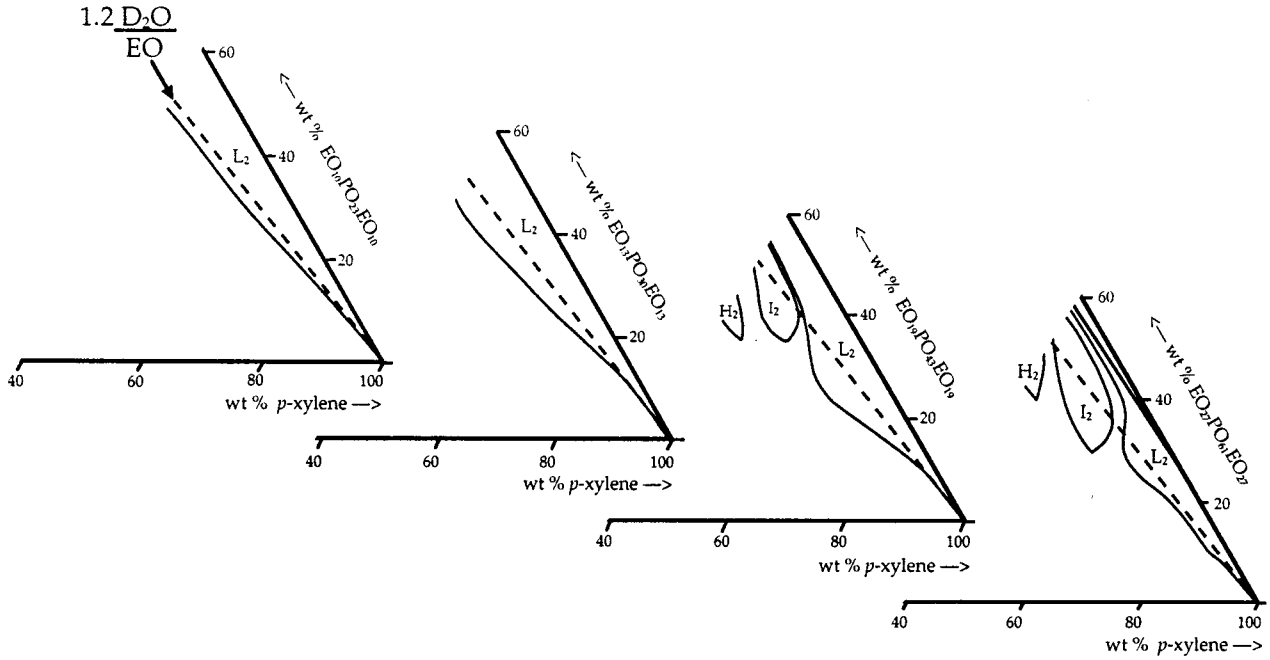

Figure 1. Partial phase diagrams of block copolymers L44, $(EO)_{10}(PO)_{23}(EO)_{10}$; L64, $(EO)_{13}(PO)_{30}(EO)_{13}$; P84, $(EO)_{19}(PO)_{43}(EO)_{19}$; and P104, $(EO)_{27}(PO)_{61}(EO)_{27}$, in D_2O and *p*-xylene at 25 °C (adapted from refs 17−19). The dashed dilution lines, corresponding to 1.2 water molecules per EO segment, are shown in the respective phase diagram. The notations for the phases are as follows: L_2, reverse micellar solution; I_2, reverse micellar cubic; and H_2, reverse hexagonal.

(water-in-oil) hexagonal phase as the only mesophases. For higher molecular weights we find a "richer" phase behavior in the ternary phase diagrams. In particular, one may find the whole spectrum of phases and structures from normal (oil-in-water) to reverse (water-in-oil) micelles in the isothermal ternary phase diagram Pluronic P84/D_2O/*p*-xylene (this phase diagram contains nine different phases).[18] This is different from the behavior of short-chained surfactants, which can be described as having a preferred or spontaneous curvature that limits the structural morphology[20] but is reminescent of block copolymer phase behavior.[18]

The oil-rich solution phase (L_2 phase) can solubilize a certain amount of water, typically 2−3 water molecules per EO segment of the copolymer. The water-induced micellization occurs at approximately 0.2 water molecules per EO segment for copolymer L64.[11] (For the L64 copolymer in mixtures with water and *o*-xylene, Chu et al have made extensive studies by for example scattering and NMR.[11,21−24]) To further understand the self-association properties of block copolymers in selective solvents, and in particular the molecular weight dependence of micellization and further ordering into a cubic lattice, we have here studied the structure of the reverse micelles formed in the L44, L64, P84, and P104 systems with water and *p*-xylene using small-angle neutron scattering (SANS). To compare different molecular weights, we have focused on a particular oil dilution line with a constant 1.2 water molecules per EO segment. The dilution lines are indicated in the partial phase diagrams of the four investigated systems which are presented in Figure 1. For the higher molecular weight copolymers, P84 and P104, the reverse micelles on this dilution line crystallize at higher concentrations into cubic phases. These phases are also of particular interest since they are very rare in low molecular weight surfactant systems while appearing to be a commonly formed phase with block copolymers.

This paper is organized as follows. After a section on experimental conditions, we present the scattering data that were recorded using two different contrasts. We then proceed to analyze the micellar dimensions using a simple core shell model of the micellar aggregates. While this model captures the salient features of the micellar form factor at lower values of the scattering vector, q, deviation occurs at higher q where the scattering is dominated by the local copolymer structure. Finally, we summarize the effect of molecular weight and micellar concentration and briefly address the effect of temperature. For comparison, we also present some data on normal (oil-in-water) micelles.

2. Experimental Section

2.1. Materials and Sample Preparation. The triblock poly(ethylene oxide)−poly(propylene oxide)−poly(ethylene oxide) ($(EO)_x(PO)_y(EO)_x$) copolymers were obtained as a gift from BASF Corp., New Jersey. The trade names and the molecular formulas are as follows: Pluronic L44, $(EO)_{10}(PO)_{23}(EO)_{10}$; Pluronic L64, $(EO)_{13}(PO)_{30}(EO)_{13}$; Pluronic P84, $(EO)_{19}(PO)_{43}(EO)_{19}$; Pluronic P104, $(EO)_{27}(PO)_{61}(EO)_{27}$. According to the manufacturer, the nominal molecular weight of the copolymers used are 2200, 2900, 4200, and 5900, and the PEO content is 40 wt %. These materials are slightly polydisperse. Wu et al.[11] found a value of 1.1 for the ratio M_w/M_n of L64, where M_w and M_n are the weight-averaged and number-averaged molecular weight, respectively. Minor amounts of hydrophobic impurities have been found in L64.[25,26] Presumably the other copolymers have similar polydispersities and impurities, but on this there are no data available. We made no attempts to purify the copolymers that were used as received. Deuterated water (D_2O, 99.80 at. % ^2H) and deuterated *p*-xylene ($C_6D_4(CD_3)_2$, >99.00 at. % ^2H) were purchased from Dr. Glaser AG, Basel, Switzerland. The densities (at 25 °C) of the block copolymer, D_2O, H_2O, and *p*-xylene-d_{10} are 1.05, 1.11, 0.998, and 0.94 g/mL, respectively. The molar volume of the copolymers, $\nu_{p,i}$ (where i = L44, L64, P84, and P104), calculated from the densities and the molecular weights, are $\nu_{p,L44} = 3500$ Å^3, $\nu_{p,L64} = 4600$ Å^3, $\nu_{p,P84} = 6700$ Å^3, and $\nu_{p,P104} = 9400$ Å^3. The samples were prepared by weighing appropriate amounts of block copolymer, water, and oil. Two sets of samples were prepared, one with protonated water and one with a mixture of 8 wt % protonated water and 92 wt % deuterated water, to achieve neutron scattering length density matching with *p*-xylene-d_{10}. The

samples were then centrifuged in both directions repeatedly in order to mix the components. They were then kept at 25 °C to equilibrate for a few days before they where injected using a syringe to 1 mm thick quartz containers used in the experiments. The sample holder was temperature controlled.

2.2. Small-Angle Neutron Scattering (SANS). The SANS experiments were performed at Risø National Laboratory, Denmark, at a constant temperature of 22 °C (some experiments were also performed at 45 °C). Three different detector settings (6, 3, and 1 m) and three neutron wavelengths, λ (9.0, 5.7, and 2.8 Å), were used to cover scattering vectors, q ($q = (4\pi/\lambda)\sin(\theta/2)$ where θ is the scattering angle) from 0.01 to 0.5 Å^{-1}. The wavelength spread, $\Delta\lambda/\lambda$ (full width at half-maximum), was 18%. The intensity was recorded by an area detector, 128 pixels × 128 pixels. The azimuthally scattering patterns were radially averaged to one-dimensional $I(q)$ scattering functions correcting also for small inhomogeneities in the detector response.

In neutron scattering experiments one can take advantage of the very large difference in scattering length between the normal hydrogen isotope and deuterium. By exchanging hydrogen with deuterium, one may alter the contrast essentially without altering the structure. In the experiments, we worked with two different contrasts. In both cases, the oil was perdeuterated *p*-xylene-d_{10} and the copolymer was the normal protonated one. In one case, which we refer to as contrast I, the water was normal H_2O, while in the second case it was a D_2O/H_2O mixture (92 wt % D_2O, 8 wt % H_2O), having the same scattering length density as the *p*-xylene-d_{10}. The second case we refer to as contrast II. (The scattering length densities of PEO, PPO, H_2O, D_2O, and *p*-xylene-d_{10} are 0.68, 0.34, −0.56, 6.39, and 5.85 × 10^{10} cm^{-2}, respectively.[27])

At higher q (>0.2 Å^{-1}) the block copolymer micelles scatter as q^{-2}, which is similar to polymer solutions.[28,29] A constant background scattering, B, was determined from plotting $I(q)$-q^2 versus q^2, according to the relation $I(q) = A/q^2 + B$. At higher values of q^2 a linear relationship was found, and the background term, B, was evaluated from the slope. This constant term was then subtracted from the experimental spectra. The exact q dependence at high q is probably slightly less steep than q^{-2} due to stretching of the chains in the aggregated state and the high local polymer concentrations.[29] Thus, our approximation assuming a q^{-2} scaling introduces an uncertainty in the value of the background term, B. However, this influences the data only at very high q values (>0.3 Å^{-1}) and not at lower q where the intensity is several orders of magnitude higher than the background, and this is where the micellar dimensions are analyzed.

3. Results and Discussion

3.1. The SANS Data. The scattering data (on the same relative, but arbitrary, scale) from the four dilution lines and two different contrasts are presented in Figures 2 and 3a−d. Figure 2 shows the data from contrast I while the results with contrast II are presented in Figure 3. The intensities have been normalized with respect to the copolymer concentration. From these data the following general remarks can be made. The two contrasts give clearly different scattering, in particular in the intermediate q regime from 0.05 to 0.2 Å^{-1}. This demonstrates first of all that the solutions are not simply molecular dispersions but contain aggregates, of which the form factors are different in the two contrasts. The presence of aggregates can also be inferred from the strong q dependence of the scattered intensity and in particular from the presence of a pronounced correlation or structure factor peak at higher concentrations. As expected, this correlation peak gets more pronounced at higher concentration and molecular weight, as the correlations are related to increased interactions between the copolymer chains.

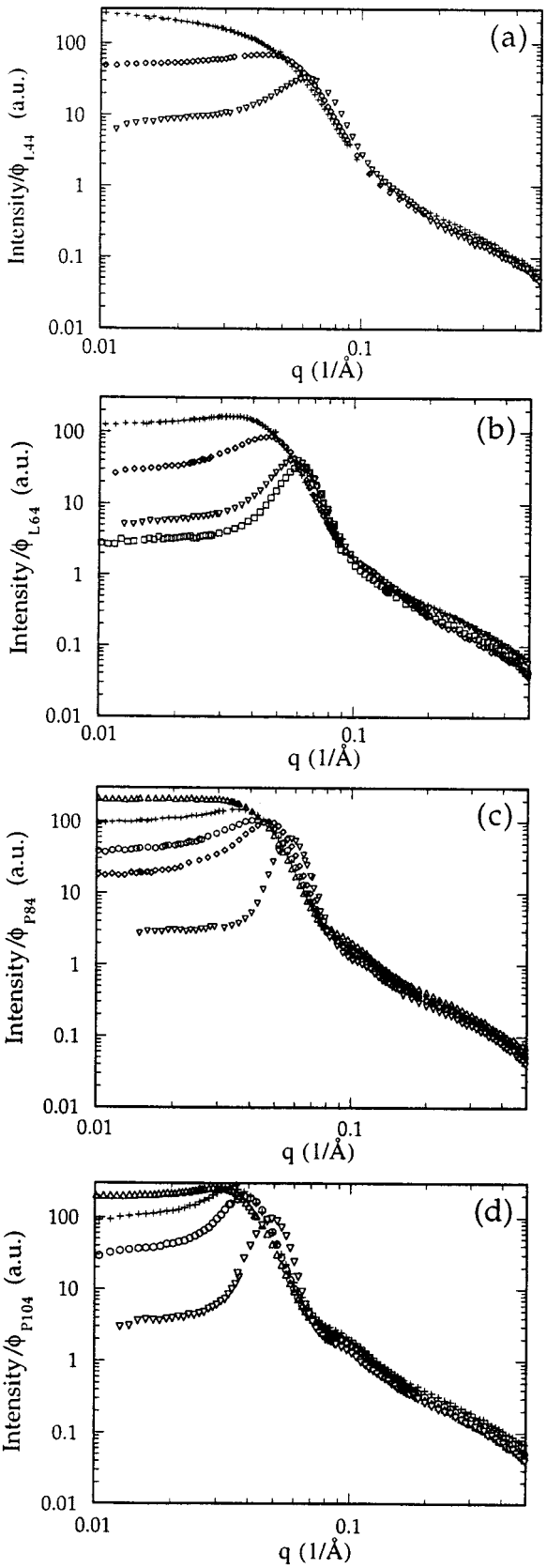

Figure 2. Concentration dependence for the case I contrast illustrated as a function of the SANS scattering normalized to the block copolymer concentration versus the scattering vector q, at 22 °C. The compositions in volume fraction block copolymer/H_2O/*p*-xylene-d_{10} are (△) 0.16/0.03/0.81, (+) 0.21/0.04/0.75, (○) 0.25/0.05/0.70, (◇) 0.30/0.06/0.64, (▽) 0.40/0.08/0.52, and (□) 0.45/0.09/0.46. SANS data are shown for four different block copolymers: (a) L44, (b) L64, (c) P84, and (d) P104.

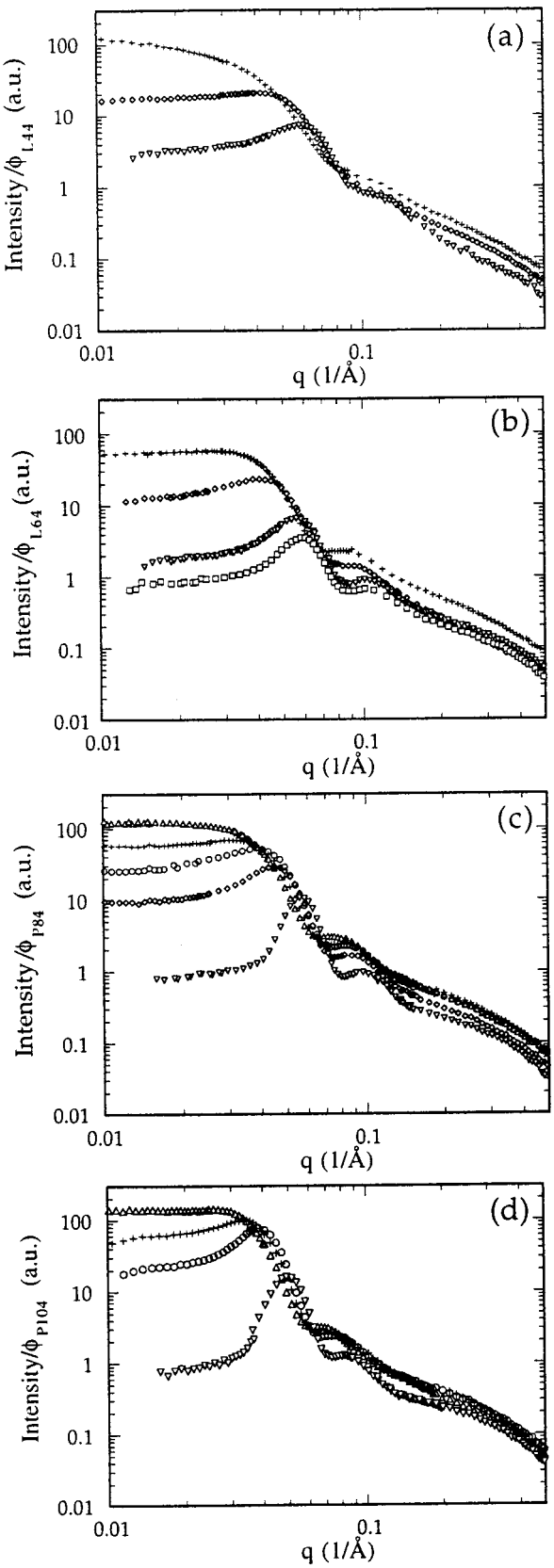

Figure 3. Concentration dependence for the case II contrast illustrated as a function of the SANS scattering normalized to the block copolymer concentration versus the scattering vector q, at 22 °C. The compositions in volume fraction block copolymer/(92 wt % D_2O:8 wt % H_2O)/*p*-xylene-d_{10} are (△) 0.16/0.03/0.81, (+) 0.21/0.04/0.75, (○) 0.25/0.05/0.70, (◇) 0.30/0.06/0.64, (▽) 0.40/0.08/0.52, and (□) 0.45/0.09/0.46. SANS data are shown for four different block copolymers: (a) L44, (b) L64, (c) P84, and (d) P104.

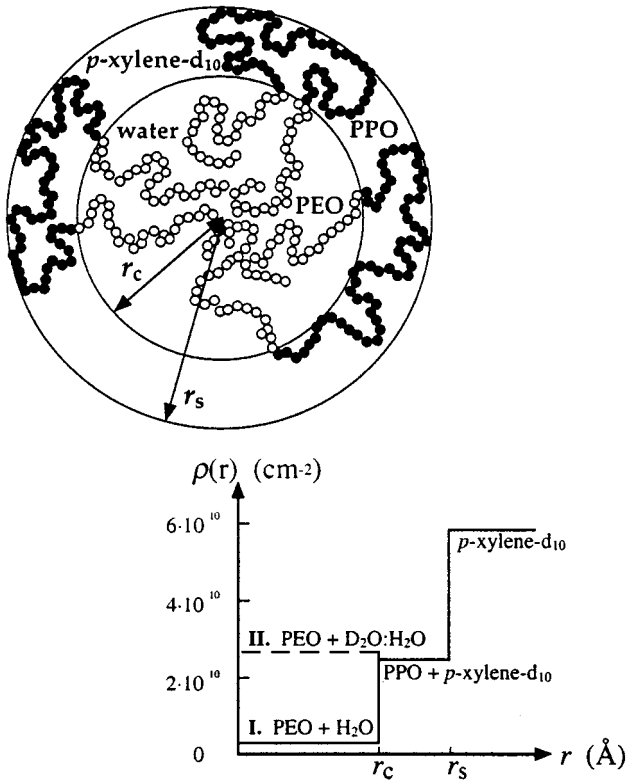

Figure 4. Schematic picture of the model of the two-sphere micelle with the water and the PEO in the core and the *p*-xylene-d_{10} solvated PPO chains in the corona. The radius of the core is given by r_c, and the outer sphere radius is given by r_s. The core−shell scattering length density profiles corresponding to the two contrasts I and II are also illustrated as a function of the radius of the micelle.

At higher q the scattered intensity decays approximately as q^{-2}. There are several possible explanations for such a scaling, but here it is most likely due to the "internal structure" of the micellar aggregates which can be viewed locally as polymer solutions (this will be discussed below). Apart from the low-q part where the scattering is strongly influenced by intermicellar interactions, the scattering curves do not change significantly with increasing concentration. This demonstrates that the reverse micellar size and shape are essentially concentration-independent.

3.2. Theoretical Considerations. *3.2.1. Form Factor of the Core−Shell Sphere.* The simplest possible micellar model with which we can test the experimental data is the core−shell sphere model. This consists of a spherical core of radius, r_c, and covered by a shell of constant thickness, $r_s - r_c$, to give an outer radius of r_s. Here we would picture the reverse micelles as PEO and water filling up the core and the shell to be made up from PPO solvated by "penetrating" *p*-xylene, as illustrated in Figure 4. In this case our two contrasts correspond to two different scattering length densities of the core, while the rest remains unaltered. The core−shell scattering length density profiles corresponding to the two contrasts, I and II, are also schematically illustrated in Figure 4.

By assigning homogeneous scattering length densities for the core and the shell, we ignore the internal polymer solution structure, and we therefore expect the model to break down at higher q. For q smaller than the inverse correlation length of the internal structure, the core and the shell will appear as uniform in the

densities. The form factor of a core−shell sphere is given by

$$P_{c-s}(q) = \left((\rho_s - \rho_o)\frac{4\pi r_s^3}{3}\right)^2 \left(\frac{3j_1(qr_s)}{qr_s} - A\frac{3j_1(qr_c)}{qr_c}\right)^2 \quad (1)$$

where $j_1(qr_c)$ is the first-order spherical Bessel function

$$j_1(qr_c) = \frac{\sin(qr_c) - qr_c\cos(qr_c)}{(qr_c)^2} \quad (2)$$

and

$$A = \left(1 - \frac{\rho_c - \rho_o}{\rho_s - \rho_o}\right)\left(\frac{r_c}{r_s}\right)^3 \quad (3)$$

Here, ρ_c, ρ_s, and ρ_o are the scattering length densities of the core, shell, and solvent (oil), respectively. When comparing this form factor with the experimental data, we assume that all the block copolymer and water are present in the aggregates. This is consistent with a recent study of the copolymer self-diffusion in the L64 system.[30] At the present water-to-copolymer ratio (1.2 mol of water per mol of EO) a very low copolymer self-diffusion coefficient was observed, which shows that the monomer concentration is low (less than 1% of the total polymer concentration). The PEO/water ratio and the scattering length density of the core, $\rho(r_c)$, are thus uniquely defined, and we can calculate the values. Therefore, if all water and EO are assumed to be solubilized in the micellar core, this is equivalent to 1.2 water molecules per EO segment. The corresponding nuclear scattering length densities are in case I $\rho(r_c) = 0.25 \times 10^{10}$ cm^{-2} and in case II $\rho(r_c) = 2.7 \times 10^{10}$ cm^{-2}.

The radius of the core depends on the aggregation number, N_{agg}, i.e., the number of block copolymers per reverse micelle. If the volume of an EO segment is v_{EO} and the block copolymer contains $2x$ such segments, the relation between r_c and N_{agg} can be written as

$$\frac{4\pi r_c^3}{3} = N_{agg}2x(v_{EO} + 1.2v_w) \quad (4)$$

The shell consists of N_{agg} PPO blocks (each PPO block has a volume yv_{PO}, where y is the number of PO segments per copolymer and v_{PO} is the volume of a PO segment) plus a certain number, $N_{o,s}$, of *p*-xylene solvating the PPO blocks. The scattering length density, ρ_s, of the shell depends on the composition, i.e., the PO/*p*-xylene ratio, of the shell and can be expressed in terms of the aggregation number and the shell volume. ρ_s is given by

$$\rho_s = \frac{N_{agg}yv_{PO}\rho_{PO} + N_{o,s}v_o\rho_o}{N_{agg}yv_{PO} + N_{o,s}v_o} \quad (5)$$

where ρ_{PO} is the scattering length density of a PO segment and v_o is the volume of a *p*-xylene molecule. The denominator of eq 5 is the shell volume which can be expressed as

$$N_{agg}yv_{PO} + N_{o,s}v_o = \frac{4\pi}{3}(r_s^3 - r_c^3) \quad (6)$$

When the scattering length density of the core is fixed, this leaves only two independent variables in the model form factor, which we may choose as the core radius r_c and the volume fraction of PPO in the shell, ϕ_{POs}. (There is also a trivial proportionality constant since the experimental data were not obtained at absolute scale.) When we compared the model form factor with the data, we also included a polydispersity in terms of a Gaussian distribution in r_c with constant composition of the shell.

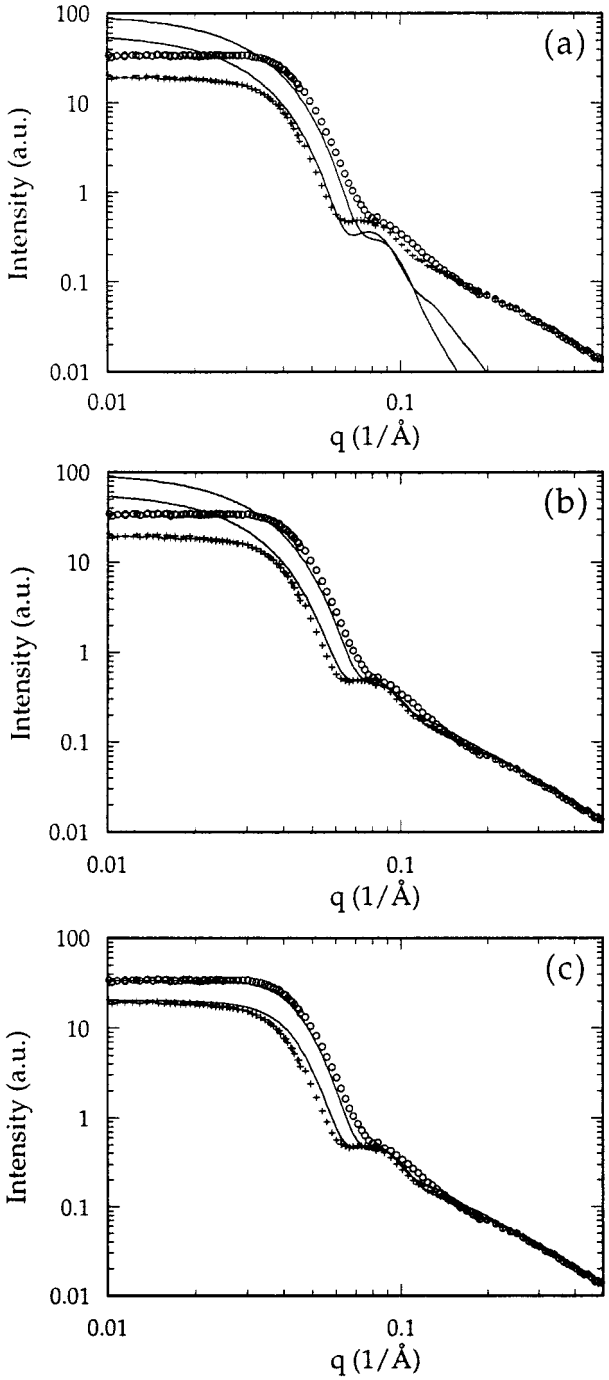

Figure 5. SANS spectra of the lowest P84 concentration (0.16/0.03/0.81 volume fraction P84/H_2O:D_2O/*p*-xylene-d_{10}) are presented for the two contrasts, case I (○) and case II (+) at 22 °C. Simulated curves of the micellar structure are shown for three cases: (a) polydisperse core and shell form factor; (b) polydisperse core and shell form factor plus the scattering from Gaussian chains; (c) polydisperse core and shell form factor plus the scattering from Gaussian chains and structure factor of homogeneous spheres.

3.2.2. Simulation with the Core−Shell Model. Figure 5a shows the scattering obtained from the two contrasts

Table 1. Results from Simulating the Scattering Spectra of Cases I and II Simultaneously to the Form Factor of a Polydisperse Two-Sphere (15−18% in the Core Radius), Plus Gaussian Chains

polymer	ϕ_p[a]	ϕ_w[a]	ϕ_{oil}[a]	$\langle r_c \rangle$[b] (Å)	$\langle r_s \rangle$[c] (Å)	ϕ_{POs}[d]	N_{agg}[e]	a_p[f] (Å^2)
L44	0.204	0.041	0.756	43	59	0.7	167	71
L44	0.295	0.062	0.064	39	56	0.6	126	79
L64	0.204	0.042	0.755	48	66	0.65	175	84
L64	0.298	0.061	0.640	45	64	0.6	150	89
P84	0.162	0.033	0.805	52	72	0.65	158	112
P84	0.207	0.042	0.752	51	69	0.7	142	116
P84	0.251	0.051	0.698	51	69	0.7	142	116
P104	0.163	0.035	0.803	58	81	0.6	147	145
P104	0.205	0.042	0.753	57	78	0.6	120	175

[a] Volume faction of the copolymer, water, and *p*-xylene, respectively. [b] $\langle r_c \rangle$ is the mean core radius of the sphere. [c] $\langle r_s \rangle$ is the mean shell radius. [d] ϕ_{POs} is the volume fraction of PPO in the shell. [e] N_{agg} is the aggregation number of the micelle. [f] a_p is the interfacial area per PEO block.

from a sample containing the copolymer Pluronic P84 at the lowest volume fraction of the copolymer, $\phi_{P84} = 0.16$. The lines correspond to the best fit (judged by the eye) from a set of simulated average form factors. The parameters are $r_c = 45$ Å, $\phi_{POs} = 0.7$, and the relative standard deviation $\sigma/\langle r_c \rangle = 0.17$. (Note that the r_c corresponds to the peak maximum in the Gaussian distribution function. The average core radius, $\langle r_c \rangle$, will be discussed below.) As is seen, this model describes the scattering in the intermediate q regime, and we capture the two different contrasts with the same structural parameters. At higher q the core−shell model is incapable of describing the experimental data. Here, the scattered intensity decays approximately as q^{-2} while the core−shell model form factor decays as q^{-4}. This is due to the assumption of homogeneous scattering length densities in the core−shell model that no longer holds at higher q, and we see the scattering from polymer chains in a solvent.

Pedersen and Gerstenberg have analyzed the scattering from polymer-coated spheres as a model for block copolymer micelles.[28] Their model form factor consists of four terms: one from the homogeneous sphere and one from the chains that were assumed to obey Gaussian statistics. The two additional terms are chain−chain and chain−sphere cross terms. The contribution from the cross terms is however small and may to a first approximation be omitted. The internal polymer−solvent structure may thus be taken into account by simply adding the form factor of flexible chains with Gaussian statistics which is given by the Debye function[31]

$$P_{chain} = 2(\rho_{chain} - \rho_{solvent})^2 \left(\frac{\exp(-u) + u - 1}{u^2} \right) \quad (7)$$

to the core−shell form factor. Here, $u = (R_g q)^2$, R_g being the radius of gyration. In the experiments, the concentration of PEO chains in the core of the micelle is 64 vol % if all water and PEO are solubilized in the core. The volume fraction of PPO in the shell was determined to ≈70 vol %. In the Gaussian chain part of the simulated scattering function we have used $R_g = 10$ Å and a polymer concentration corresponding to the PPO concentration. Note that the R_g value is only an effective one since we are approximating the locally concentrated polymer environment with Gaussian chains. However, this approximation allows us to capture the salient features of the scattering behavior.

We note also that the scattered intensity at high q is approximately the same in contrasts I and II. This implies that the scattering at high q could essentially be due to the solvated PPO in the micellar corona. (If both the PEO blocks and the PPO blocks scatter as individual chains, we expect the two contrasts to be different at high q.) However, the subtracted backgrounds are different in the two sets of samples at constant copolymer concentration. The background for the samples with the D_2O/H_2O mixture was larger than for the samples were H_2O was used as solvent. This indicate that the scattering from the core has been subtracted as a constant term in the case II contrast which could be the case if the apparent R_g is small.

The lines in Figure 5b show the simulated scattering functions when the form factor of Gaussian chains has been added to the core−shell form factor. As is seen, the lines describe the experimental data well. The simulated scattering functions correspond to $R_g = 10$ Å if we let the concentration of Gaussian chains be equal to the PPO concentration and assume uniform chain density in the shell and that we see no scattering from the PEO block in the core of the micelle.

At lower q the scattered intensity is lowered due to the intermicellar correlations. In principle, this could also be taken into account. An effective structure factor can be defined as

$$S_{eff}(q) = \frac{I(q)}{N\langle P(q) \rangle} \quad (8)$$

where N is the number density of micelles and $\langle P(q) \rangle$ is the form factor averaged over the size distribution. This is, however, not trivial. For polydisperse spheres the size polydispersity may also introduce a so-called optical polydispersity. For example, a distribution of polydisperse spherical shells has a different $S_{eff}(q)$ than that of homogeneous spheres of the same size distribution function. If we ignore this complexity and simply include a structure factor of monodisperse hard spheres, for which an analytical expression exists,[32,33] the low-q part can also be reasonably well described as is seen by the lines in Figure 5c. Here, the hard sphere volume fraction is 0.15 and the hard sphere radius is 65 Å, which are reasonable values. The position of the intensity maximum, which approximately varies as $\phi^{-1/3}$, obtained at higher concentrations, is roughly consistent with the same hard sphere radius. However, the experimental structure factor peaks are much less sharp than what is predicted for monodisperse hard spheres. Apart from polydispersity effects, we also expect some broadening of the structure factor peak due to a softer pair interaction than hard spheres.[29]

3.3. Discussion of the Results from the Simulation. In Table 1 we have summarized the results of $\langle r_c \rangle$,

$\langle r_s \rangle$, and ϕ_{POs} for the different copolymer molecular weights and micellar concentrations, as deduced from comparison between simulated and experimental scattering data. Only data for $\phi_p \leq 0.3$ are presented since the interactions between the micelles are very strong at higher concentrations, and the simulation becomes very uncertain as the structure factor is not known in detail. The interfacial area, a_p, per PEO block at the polar−apolar interface between the core and the shell deduced from the core radius and sample composition is also shown in Table 1. The area can be written as

$$a_p = \frac{3(1-f)v_p}{2\phi_p\langle r_c \rangle} \tag{9}$$

where $(1 - f) = \phi_{PEO} + \phi_w$. This is the polar volume fraction ($\phi_{PEO} = 0.38\phi_p$, where ϕ_p is the copolymer volume fraction. The PEO block that makes up ≈40 wt % of the molecular weight makes up ≈38 vol % of the copolymer.) Since the (average) area per PEO block is defined as the total interfacial area divided by the total number of PEO blocks (twice the number of copolymer chains), the core radius that enters in eq 9 should not be the radius corresponding to the peak in the assumed Gaussian size distribution function (the r_c). Rather, $\langle r_c \rangle$ is the radius that monodisperse spheres would have if the area per PEO block is a_p. We thus need to consider the volume-to-area ratio of the aggregates, and hence the average radius is given by

$$\langle r_c \rangle = \frac{3\langle V_c \rangle}{\langle A_c \rangle} = \frac{3\int dr_c\ r_c^3 P(r_c)}{\int dr_c\ r_c^2 P(r_c)} \tag{10}$$

where $P(r_c)$ is the radius distribution function. The $\langle r_s \rangle$ is given from $\langle r_c \rangle$, or more correctly from the distribution of aggregation numbers, since we have assumed constant solvation of the PPO (corresponding to a constant scattering length density of the domain). The aggregation numbers given in Table 1 are calculated from eq 4 using the $\langle r_s \rangle$ as core radius, r_s.

If we now look in Table 1, as expected, the general trend is that the core and shell radii increase with increasing block copolymer molecular weight. The area per PEO block obtained using eqs 9 and 10 is consistent with the values obtained previously, from small-angle X-ray scattering data, in the nearby reverse hexagonal and lamellar phases.[17−19] The molecular weight dependence on the core radius is relatively small ($\langle r_c \rangle \propto v_p^{1/3} \approx M_w^{1/3}$). This corresponds to an interfacial area that scales with molecular weight as $a_p \propto M_w^{2/3}$. In the lamellar phase the a_p is scaling with molecular weight as $a_p \propto M_w^{1/2}$, i.e., scaling as Gaussian chains.[34] The aggregation number determined for the Pluronic L64 agree with a light scattering study by Chu et al.[11] Because of this weak micellar growth and increased area per polymer, we hardly see any molecular weight dependence in the position of the intensity maximum (Figure 2).

The determined core radii decreases slightly with increasing micelle concentration. However, at higher concentrations the uncertainties in $\langle r_c \rangle$ and $\langle r_s \rangle$ become higher due to the increasing influence of the structure factor, which is not known in detail. The decrease in radius could also be due to the fact that we are observing a minor growth of the micelles into prolate shapes. It is well-known that a model of polydisperse spheres can well describe the scattering, for example, from prolates if the axial ratio is not too different from one. In fact, an analysis of scattering data in terms of polydisperse spheres gives a decreasing apparent average radius and an increasing apparent polydispersity when spheres turn into prolates. A minor growth into prolates would also be consistent with the fact that the reverse micellar cubic phases of the P84 and P104 systems do not seem to consist of a simple fcc or bcc packing of spheres but rather a more complex cubic packing.[18,19]

The triblock Pluronic copolymer may form bridges between two adjacent micelles by having one PEO block in each micelle which could lead to a sample spanning network. Such a network was for example observed by Bagger-Jörgensen et al.[35] in a system where hydrophobically end-modified poly(ethylene oxide) was mixed with normal micelles in an aqueous solution. However, in the present L_2 phase the viscosities are not particularly high, which means that if bridges are formed they must have a very short lifetime, which in principle can be expected since the polymer segregation is not very strong here. Neither do we see evidence of bridging in the scattering profiles. Strong bridging results in an effectively attractive interaction between the micelles, which in turn results in intense scattering at low q.[35] This is not observed here.

3.4. Temperature Dependence. We have also recorded the scattering at a higher temperature of 45 °C. In all cases the results are very similar to that at 22 °C. In other words, the temperature dependence is weak. To illustrate this, we compare in Figure 6 the scattering from two samples in the P84 system at the two different temperatures using contrast II. Here, as in all samples, there is a slight increase (≤10%) in the apparent micellar radius.

3.5. The Normal Micellar Region, the L_1/I_1 Phase. The SANS study in this report is concentrated on the oil continuous region, but a few samples with varied molecular weight were analyzed in the water continuous region. Here we would picture the normal micelles as PPO filling up the core (as no oil is added) and the shell to be made up from PEO solvated by deuterated water. Several studies of the structure of the PEO−PPO−PEO block copolymers in aqueous solution have been made. (See for example ref 2 and references therein.) The micellar size for copolymer P84, P104, and P85 (P85 = $(EO)_{25}(PO)_{40}(EO)_{25}$ in ref 3, P85 = $(EO)_{27}(PO)_{39}(EO)_{27}$ in ref 4) in water solution is almost independent of copolymer concentration but depends on the temperature.[3,4,7] The concentration dependence is thus the same as we observed in this report in the reverse micellar phase. The temperature dependence on the core radius is lower in the reverse micellar phase (≈25% in the L_1 phase[3,4] compared to ≤10% in the L_2 phase, in the temperature interval 22−45 °C). This is most likely due to the changes in polarity of the PEO with temperature. In the L_1 phase where the amount of water per EO segment is high, increased temperature leads to less water per EO segment, less repulsion between the PEO blocks in the micelle corona, and higher aggregation numbers.[5,7] In the L_2 phase the water content per EO segment is much less, and at the same time, the solvation (and repulsion) of the PPO blocks forming the corona is not affected to the same extent as in the PEO/water case; therefore, the aggregation number is less influenced by temperature changes.

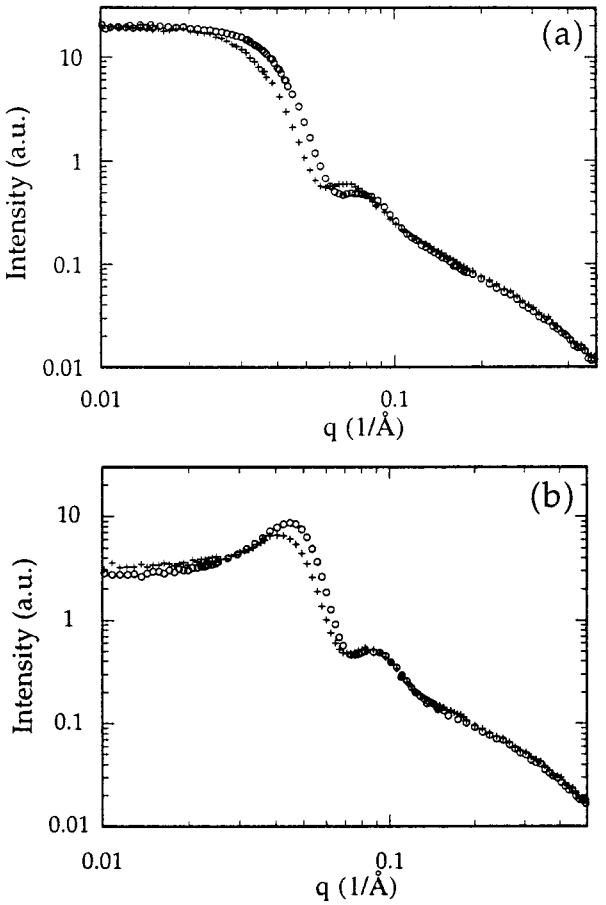

Figure 6. Scattering from two samples in the P84 system at the two different temperatures, 22 °C (○) and 45 °C (+), using contrast II. The concentrations are (a) 16 vol % copolymer P84, 3 vol % D_2O:H_2O mixture and 81 vol % *p*-xylene-d_{10} and (b) 30 vol % copolymer P84, 6 vol % D_2O:H_2O mixture and 64 vol % *p*-xylene-d_{10}.

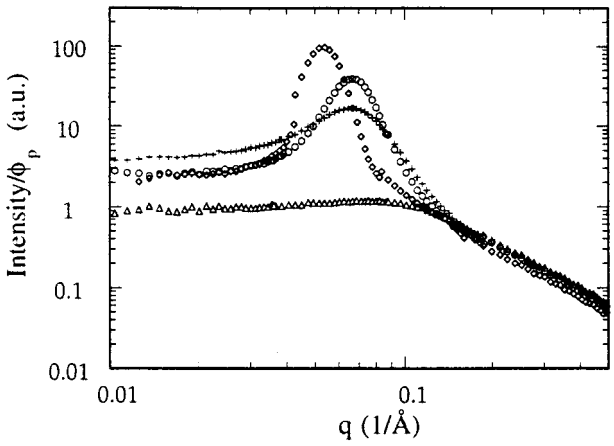

Figure 7. SANS spectra in the normal (oil-in-water) region at 22 °C. The concentrations are 36 vol % copolymer and 64 vol % D_2O. The copolymers are L44 (△), L64 (+), P84 (○), and P104 (◇).

The dependence in the normal micelle structure of the block copolymer molecular weight is shown in Figure 7 for samples with 36 vol % copolymer and 64 vol % deuterated water. From these data the following general remarks can be made. The scattering shows strong q dependence particular in the intermediate q regime from 0.04 to 0.1 Å^{-1}. The strong q dependence of the scattered intensity and the presence of a pronounced correlation peak for all copolymers but the one with the lowest molecular weight demonstrates that the solutions are not simply molecular dispersions but contain micelles. The scattering curve for L44 indicates that the monomer concentration is very high. The cmc for this copolymer in not known. However, if we use published data for the other PEO−PPO−PEO block copolymers,[36] we can estimate the cmc to be ≈20 wt %. The interaction increases with increasing molecular weight as is seen from the correlation peak. This is consistent with the fact that the micelles in the P84 and the P104 copolymer systems crystallize into normal micellar cubic phases.[18,19]

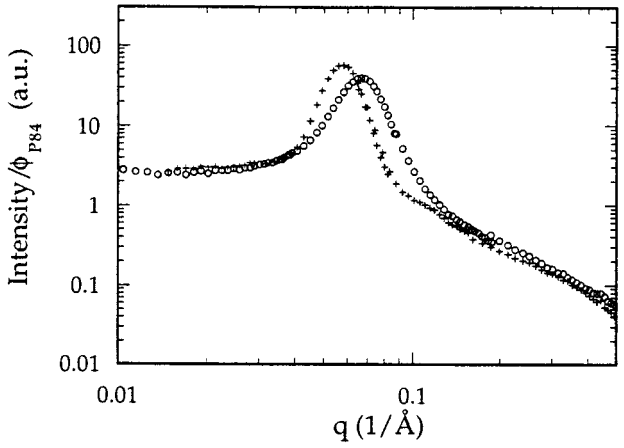

Figure 8. Comparison between the SANS scattering spectra normalized to copolymer concentration from a normal micellar cubic I_1 sample and a reverse micellar cubic I_2 sample, of the copolymer P104 at 22 °C. The spectra are I_1 0.36/0.64 volume fraction P104/D_2O (○) and I_2 0.40/0.08/0.52 volume fraction P104/H_2O/*p*-xylene-d_{10} (+).

The size of the micelles changes with molecular weight, but this change is small. These are the same conclusions as we drew in the oil continuous region. If we compare the micellar size in the L_1 phase with that in the L_2 phase at the same volume fraction of the enclosed phase (f in the L_1 phase and $1 - f$ in the L_2 phase) and approximately the same copolymer concentration, we find that the sizes are generally slightly larger in the L_2 phase. This is consistent with the general trend that the interfacial area per PEO block is slightly smaller on the oil-rich side compared to the water-rich side of the phase diagram. The difference is however small (≈10%), and structure and phase equilibrium are approximately symmetric around $f = {}^1/_2$. This symmetry, which these systems share in common with the one component block copolymer melts, has been discussed for the phase diagrams.[34] This is also seen in Figure 8, where we compare the scattering from a sample from the I_1 phase with that from a sample in the I_2 phase in the P104 system. The volume fraction of the enclosed phase, f in the I_1 sample, equals $1 - f$ in the I_2 sample (=0.22), and the copolymer concentrations are similar. The I_1 sample contains polymer micelles in D_2O, while in the I_2 sample the micelles contain copolymer and H_2O which are dissolved in *p*-xylene-d_{10}. Contrast conditions are therefore very similar. As is seen in Figure 8, the two scattering curves almost coincide, demonstrating that the structures in the two samples are very similar.

4. Summary

Poly(ethylene oxide)−poly(propylene oxide)−poly(ethylene oxide) (PEO−PPO−PEO) block copolymers self-assemble in the presence of selective solvents water

and *p*-xylene to form (among others) reverse (water-in-oil) micelles in an oil continuous solution. These reverse micelles can order into a cubic structure upon an increase of their volume fraction for block copolymers of sufficiently high molecular weight. We set out to study the microstructure (form and dimension) as the reverse micelles order with increasing block copolymer volume fraction (at a fixed water/block copolymer ratio) and with increasing block copolymer molecular weight (at the same architecture and PEO/PPO block ratio), at two different temperatures, using SANS with solvent contrast variation.

The scattering behavior indicates that the micelles are approximately spherical but polydisperse. We used a two-sphere model, assuming that all the PEO and water are in the micelle core and that PPO with *p*-xylene forms a solvated shell. Good agreement with the scattering data was achieved when the form factor of Gaussian chains was added to the core−shell form factor.

The micellar radius is found to increase with increasing the block copolymer molecular weight and the solution temperature, and it is approximately independent of the micelle concentration (at a fixed water/EO ratio) for the composition range examined. These trends are similar to the ones observed for PEO−PPO−PEO micelles in aqueous solutions (normal or oil-in-water micelles). The temperature dependence on the core radius is lower in the reverse micellar phase. For the same volume fraction of the enclosed phase (PEO + water for reverse micelles and PPO for normal micelles), we found that the micellar sizes are generally larger in the oil continuous solution. This is consistent with the general trend that the interfacial area per PEO block is slightly smaller on the oil-rich side compared to the water-rich side of the phase diagram.

Acknowledgment. This work was supported by the Swedish Natural Science Research Council (NFR) and the Center of Competence for Amphiphilic Polymers from Renewable Resources, Lund University, Sweden. Stimulating and helpful discussions with Jan Skov Pedersen and Bernard Cabane and the European TMA program for large facilities are kindly acknowledged.

References and Notes

(1) Alexandridis, P. *Curr. Opin. Colloid Interface Sci.* **1997**, *2*, 478.
(2) Mortensen, K. *Curr. Opin. Colloid Interface Sci.* **1998**, *3*, 12.
(3) Mortensen, K.; Pedersen, J. S. *Macromolecules* **1993**, *26*, 805.
(4) Mortensen, K.; Brown, W. *Macromolecules* **1993**, *26*, 4128.
(5) Mortensen, K. *J. Phys.: Condens. Matter* **1996**, *8*, A103.
(6) Goldmints, I.; von Gottberg, F. K.; Smith, K. A.; Hatton, T. A. *Langmuir* **1997**, *13*, 3659.
(7) Liu, Y.; Chen, S.-H.; Huang, J. S. *Macromolecules* **1998**, *31*, 2236.
(8) Mitchell, D. J.; Tiddy, G. J. T.; Waring, L. *J. Chem. Soc., Faraday Trans. 1* **1983**, *79*, 975.
(9) Wanka, G.; Hoffmann, H.; Ulbricht, W. *Macromolecules* **1994**, *27*, 4145.
(10) Alexandridis, P.; Zhou, D.; Khan, A. *Langmuir* **1996**, *12*, 2690.
(11) Wu, G.; Zhou, Z.; Chu, B. *Macromolecules* **1993**, *26*, 2117.
(12) Alexandridis, P.; Andersson, K. *J. Phys. Chem. B* **1997**, *101*, 8103.
(13) Zhou, S.; Su, J.; Chu, B. *J. Polym. Sci., Part B: Polym. Phys.* **1998**, *36*, 889.
(14) Karlström, G. *J. Phys. Chem.* **1985**, *89*, 4962.
(15) Kahlweit, M.; Strey, R.; Busse, G. *J. Phys. Chem.* **1990**, *94*, 3881.
(16) Olsson, U.; Jonströmer, M.; Nagai, K.; Söderman, O.; Wennerström, H.; Klose, G. *Prog. Colloid Polym. Sci.* **1988**, *76*, 75.
(17) Alexandridis, P.; Olsson, U.; Lindman, B. *Macromolecules* **1995**, *28*, 7700.
(18) Alexandridis, P.; Olsson, U.; Lindman, B. *Langmuir* **1998**, *14*, 2627.
(19) Svensson, B.; Alexandridis, P.; Olsson, U. *J. Phys. Chem. B* **1998**, *102*, 7541.
(20) Olsson, U.; Wennerström, H. *Adv. Colloid Interface Sci.* **1994**, *49*, 113.
(21) Wu, G.; Zhou, Z.; Chu, B. *J. Polym. Sci., Part B: Polym. Phys.* **1993**, *32*, 2035.
(22) Wu, G.; Chu, B. *Macromolecules* **1994**, *27*, 1766.
(23) Wu, G.; Chu, B.; Schneider, D. K. *J. Phys. Chem.* **1994**, *98*, 12018.
(24) Chu, B.; Wu, G. *Macromol. Symp.* **1995**, *90*, 251.
(25) Zhou, Z.; Chu, B. *Macromolecules* **1988**, *21*, 2548.
(26) Kositza, M. J.; Bohne, C.; Alexandridis, P.; Hatton, T. A.; Holzwarth, J. F. *Langmuir* **1999**, *15*, 322.
(27) Cabane, B. In *Small Angle Scattering Methods*; Marcel Dekker: New York, 1987; p 57.
(28) Pedersen, J. S.; Gerstenberg, M. C. *Macromolecules* **1996**, *29*, 1363.
(29) Gast, A. P. *Langmuir* **1996**, *12*, 4060.
(30) Barreleiro, P. A.; Andersson, K.; Håkansson, B.; Olsson, U.; Alexandridis, P., to be submitted for publication.
(31) Debye, P. *J. Phys. Colloid Chem.* **1947**, *51*, 18.
(32) Percus, J. K.; Yevick, G. J. *Phys. Rev.* **1958**, *110*, 1.
(33) Ashcorft, N. W.; Lekner, J. *Phys. Rev.* **1966**, *145*, 83.
(34) Svensson, B.; Olsson, U.; Alexandridis, P., manuscript in preparation.
(35) Bagger-Jörgensen, H.; Coppola, L.; Thuresson, K.; Olsson, U.; Mortensen, K. *Langmuir* **1997**, *13*, 4204.
(36) Alexandridis, P.; Holzwarth, J. F.; Hatton, T. A. *Macromolecules* **1994**, *27*, 2414.

MA990079W